


ORIGINAL ARTICLE

OPEN

VLDL lipidomics reveals hepatocellular lipidome changes in metabolic dysfunction–associated steatotic liver disease

David Guardamino Ojeda¹  | Yusuf Yalcin² | Yered Pita-Juarez³ | Aaron Hakim^{1,4} | Susmita Bhattarai¹ | Zsu-Zsu Chen⁵ | John M. Asara⁶ | Margery A. Connelly⁷ | Melissa R. Miller⁸ | Michelle Lai¹ | Z. Gordon Jiang¹

¹Division of Gastroenterology, Department of Medicine, Beth Israel Deaconess Medical Center, Harvard Medical School, Boston, Massachusetts, USA

²Department of Internal Medicine, Steward Carney Hospital, Tufts University School of Medicine, Dorchester, Massachusetts, USA

³Department of Pathology, Beth Israel Deaconess Medical Center, Harvard Medical School, Boston, Massachusetts, USA

⁴Divisions of Genetics and Cardiovascular Medicine, Department of Medicine, Brigham and Women's Hospital, Harvard Medical School, Boston, Massachusetts, USA

⁵Division of Endocrinology, Beth Israel Deaconess Medical Center, Harvard Medical School, Boston, Massachusetts, USA

⁶Division of Signal Transduction, Department of Medicine, Beth Israel Deaconess Medical Center, Harvard Medical School, Boston, Massachusetts, USA

⁷Labcorp, Morrisville, North Carolina, USA

⁸Pfizer Inc., Cambridge, Massachusetts, USA

Correspondence

Z. Gordon Jiang, Division of Gastroenterology, Beth Israel Deaconess Medical Center, Harvard Medical School, 99 Brookline Ave, RN-0236, Boston, MA 02115, USA.
Email: zgjiang@bidmc.harvard.edu

Michelle Lai, Division of Gastroenterology, Beth Israel Deaconess Medical Center, Harvard Medical School, 330 Brookline Ave, LMOB4A, Boston, MA 02215, USA.
Email: mlai@bidmc.harvard.edu

Abstract

Background: The production of VLDL is one of the primary mechanisms through which liver cells regulate intracellular lipid homeostasis. We hypothesize that the disease characteristics of metabolic dysfunction–associated steatotic liver disease (MASLD) differentially impact VLDL lipid composition. This study comprehensively examines the relationship between VLDL-lipidome and MASLD histology and disease-associated genetics, aiming to define MASLD-related VLDL changes.

Methods: We performed untargeted lipidomics on serum VLDL particles in a cohort of biopsy-proven MASLD patients to examine the relationship between VLDL-lipidome and MASLD disease features as well as MASLD-related genetic variants.

Results: Among 1514 detected lipid species in VLDL, triglyceride (TG), phosphatidylcholine (PC), and ceramide (Cer) were the top classes. Moderate to severe hepatic steatosis was associated an increase in

Abbreviations: BIDMC, Beth Israel Deaconess Medical Center; Cer, ceramide; CE, cholesteryl ester; DG, diacylglycerol; FDR, false detection rate; HPLC, high-performance liquid chromatography; LPC, lysophosphatidylcholine; LSEA, Lipid Set Enrichment Analysis; MASLD, metabolic dysfunction–associated steatotic liver disease; MePC, monoether phosphatidylcholine; NMR, nuclear magnetic resonance; OPLS-DA, Orthogonal Partial Least Squares-Discriminant Analysis; PC, phosphatidylcholine; PCA, Principal Component Analysis; PE, phosphatidylethanolamine; PI, phosphatidylinositol; PL, phospholipid; PQN, Probability Quotient Normalization; SL, sphingolipid; SM, sphingomyelin; ST, sterol; TG, triglyceride; VLDL, very low-density lipoprotein.

David Guardamino Ojeda and Yusuf Yalcin are co-first authors.

Supplemental Digital Content is available for this article. Direct URL citations are provided in the HTML and PDF versions of this article on the journal's website, www.hepcommjournal.com.

This is an open access article distributed under the terms of the Creative Commons Attribution-Non Commercial-No Derivatives License 4.0 (CCBY-NC-ND), where it is permissible to download and share the work provided it is properly cited. The work cannot be changed in any way or used commercially without permission from the journal.

Copyright © 2025 The Author(s). Published by Wolters Kluwer Health, Inc. on behalf of the American Association for the Study of Liver Diseases.

VLDL-TG, especially those with palmitic acid (C16:0). A unified acyl chain distribution analysis revealed that steatosis was associated with increases in TGs with saturated and monounsaturated fatty acyl chains, but decreases in polyunsaturated fatty acyl chains, a pattern that was not mirrored in acyl chains from VLDL-PC or VLDL-Cer. Lobular inflammation was associated with reductions in lipids with polyunsaturated acyl chains, particularly docosahexaenoic acid (C22:6). Meanwhile, patients with advanced liver fibrosis (stages 3–4) had reductions in VLDL-TGs with both saturated and polyunsaturated acyl chains and overall enrichment in Cer species. Furthermore, MASLD-associated genetic variants in *PNPLA3*, *TM6SF2*, *GPAM*, *HSD17B13*, and *MTARC1* demonstrated distinct VLDL-lipidomic signatures in keeping with their biology in lipoprotein metabolism.

Conclusions: Hepatic steatosis and liver fibrosis in MASLD are associated with distinct VLDL-lipidomic signatures, respectively. This relationship is further modified by MASLD-genetics, suggesting a differential impact of pathogenic features on hepatocellular lipid homeostasis.

Keywords: lipidomics, lipoprotein, MASLD, *PNPLA3*, VLDL

INTRODUCTION

Metabolic dysfunction–associated steatotic liver disease (MASLD) is the leading form of chronic liver disease and a rapidly rising indication of liver transplant across the world.^[1,2] MASLD results from the accumulation of lipid droplets in hepatocytes. Due to the difficulty of accessing human hepatocytes in their native states, the changes in lipid metabolism in hepatocytes in MASLD remain elusive.

Hepatocellular lipid droplets consist of hydrophobic (also known as apolar) lipids such as triacylglycerol (TG) and cholesteryl ester in the core and amphipathic (also known as polar) lipids such as phospholipids (PLs) and sphingolipids (SLs) on the surface. Fatty acyl chains are the potentially exchangeable constituents of both apolar and polar lipids. Hepatic steatosis occurs when the combined rate of fatty acid uptake and de novo synthesis exceeds that of its oxidation in the mitochondria and export from hepatocytes.^[3] Hepatocytes produce VLDLs to export large quantities of apolar and, to a lesser extent, polar lipids into the circulation, a crucial process that modulates intracellular lipid content.^[4] The relevance of VLDL biology in MASLD is supported by the discovery of genetic variants that directly impact VLDL secretion, such as the *TM6SF2* rs58542926, encoding an E167K mutation.^[5,6] Other genetic variants may indirectly impact VLDL production. *PNPLA3* and *HSD17B13* are both lipid droplet-associated proteins. Genetic variants

in both genes have been found to be associated with hepatic steatosis, but have a differential impact on liver injury and fibrosis progression.^[7–10] We and others have identified that a loss-of-function variant in *GPAM*, a mitochondrial acyltransferase for the synthesis of TG, is associated with MASLD and liver injury.^[11,12] Meanwhile, *MTARC1*, another gene encoding an amidoxime reducing component in the mitochondrial cytochrome P450, was associated with both hepatic steatosis and circulating levels of LDL.^[13]

Mass spectroscopy–based lipidomics has emerged as a powerful tool for studying the complex lipidome in biological samples. Previous lipidomics work has studied serum/plasma samples and liver biopsies from MASLD patients.^[14] For example, Puri et al^[15] observed an increase in monounsaturated fatty acids, lipoxygenase metabolites, and a decrease in polyunsaturated fatty acids from simple steatosis to steatohepatitis in the plasma of 150 patients. However, it is not clear whether these changes resulted directly from changes in hepatocytes, as lipids in the circulation have complex origins.

Herein, we developed a VLDL-lipidomics method that can be deployed safely using serum or plasma samples to probe disease-related changes relevant to hepatocellular lipid homeostasis. This strategy leverages the unique biology of VLDL and its relationship to MASLD, which has been described by many groups in the lipoprotein research community, including ours.^[4,16,17] First, VLDL is only produced by hepatocytes and can be easily isolated from fasting serum or plasma. Secondly,

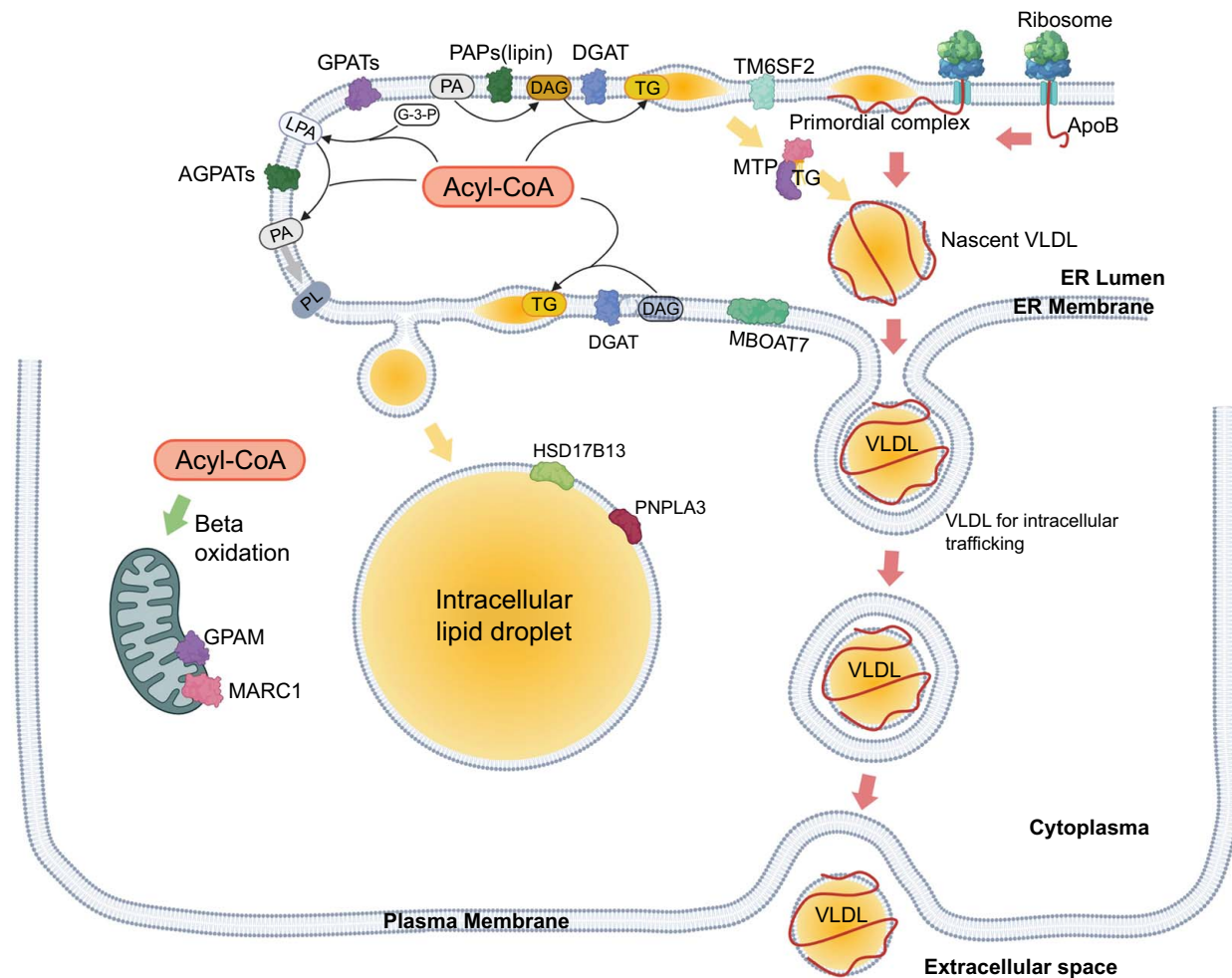


FIGURE 1 VLDL assembly in hepatocytes. The diagram illustrates VLDL assembly in hepatocytes. VLDL synthesis requires the coordination between protein and lipid synthesis. Apolipoprotein B (apoB), the main protein component of VLDL, is translated in the ER lumen to form a primordial complex. Acyl-CoA is the common substrate for the synthesis of phospholipids (PLs) and TG. Glycerol-3-phosphate acyltransferase (GPAT) converts acyl-CoA and glycerol-3-phosphate (G-3-P) to lysophosphatidic acid (LPA), which is converted to phosphatidic acid (PA) through 1-acylglycerol-3-phosphate-O-acyltransferase (AGPAT). On the one hand, PA can be used to synthesize PL. On the other hand, PA is also converted to DAG through phosphatidic acid phosphatase (PAP, also known as lipin), and TG through acyl-CoA diacylglycerol acyltransferase (DGAT). PL and TG are incorporated into intracellular lipid droplets and nascent VLDL particles through microsomal triglyceride transfer protein (MTTP) and other chaperones. MASLD-related genes, such as PNPLA3, TM6SF2, HSD17B13, and GPAM (a mitochondrial isoform of GPAT), are noted on the diagram as well. Abbreviation: ER, endoplasmic reticulum.

VLDL shares a similar structure to hepatocellular lipid droplet with an apolar lipid core derived from the lipid droplet in hepatocytes and polar lipids from the membrane of the endoplasmic reticulum (ER) and Golgi apparatus (Figure 1). Finally, VLDL has a short half-life of ~4 hours, maintaining a high lipid-composition fidelity to the cellular compartments of its origin, vis-a-vis hepatocytes.^[18]

In this study, we describe the VLDL-lipidomics of a well-characterized MASLD cohort and report disease-specific changes in main lipid classes using a novel unified acyl chain distribution analysis. This method provides a novel tool to study lipid metabolism in MASLD without the need to obtain liver tissue. It could be readily adopted in clinical studies to interrogate disease biology and potentially develop novel biomarkers.

METHODS

Patient cohorts

Patients are identified from a prospective NAFLD registry at Beth Israel Deaconess Medical Center (BIDMC) that has been previously described.^[19] Patients with a clinical diagnosis of MASLD that was confirmed by liver biopsy have been enrolled since 2009. Patients with other forms of chronic liver diseases, alternative causes for hepatic steatosis, such as medication, hereditary hemochromatosis, or consumption of > 20 g of alcohol daily, were excluded from the registry. Data on patient demographics, medical history, and physical exam were obtained at the enrollment of the study. Laboratory tests and serum

collection were performed at enrollment, while liver biopsy was performed within 3 months. A total of 162 patients with fasting serum samples at index visits were enrolled in the study. The study was conducted in accordance with the guidelines of the Declaration of Helsinki. The clinical protocol was approved by the BIDMC institutional review board, and all participants provided written informed consent.

Quantitation of VLDL by nuclear magnetic resonance spectroscopy

Concentrations of VLDL, also known as triglyceride-rich lipoproteins, were measured by nuclear magnetic resonance (NMR) spectroscopy at LabCorp.^[20] Patient serum was thawed and analyzed on a 400 MHz Vantera Clinical Analyzer to collect the proton NMR spectra. The broad peak corresponding to the lipid methyl groups was deconvoluted to separate the unique lipoprotein signals and to obtain molar concentrations for each of the lipoprotein classes and subclasses using the LP4 algorithm.^[20,21] The weighted average VLDL particle size was calculated based on the distribution of the VLDL subclasses.

VLDL isolation and VLDL-lipidomics

The method to isolate VLDL has been described previously.^[22] To prepare for VLDL-lipidomics, 120 μ L serum samples were centrifuged at 90,000 rpm at 4 °C in a TLA-120.2 rotor (Beckman) for 3 hours. The top 20 μ L samples were carefully aspirated and transferred to a new tube. Lipids were extracted by 1 \times methanol and 4 \times methyl tert-butyl ether and dried on a SpeedVac concentrator (Thermo Electron) as previously described.^[23] The lipids were further isolated by HPLC using a Cadenza C18 column (Imtakt) on an Agilent 12100 system (Agilent Technologies) coupled to a Q Exactive HF Orbitrap high-resolution mass spectrometer (Thermo Fisher Scientific) in data-dependent acquisition mode with polarity switching. Data were analyzed by LipidSearch 4.1 (Thermo Fisher Scientific) for lipid identification and relative quantification.

Genotyping

Subjects were genotyped using a high-density single-nucleotide polymorphism genotyping array (Illumina OmniExpress Exome v1.6 BeadChip). Quality control was performed to remove variants with more than 5% missing data, subjects with genotype missing rate more than 2%, low call rates, genotyped sex mismatch, excess sample heterozygosity, and related subjects (kinship value >0.0884). Sample and autosomal

single-nucleotide polymorphism call rates were >0.99. After quality control, 2 samples were excluded, and 944,287 remaining probes were available for analysis. Imputation was performed with the Haplotype Reference Consortium and 1000 Genomes phase 3 samples at the Michigan Imputation Server.^[24] Analysis was performed using plink1.9.^[25]

Statistical analysis

To convert the lipid profile to lipidome per VLDL particle, signal intensities of each lipid species were divided by the respective VLDL particle concentration determined by NMR. Lipid species with >30% missing data across the cohort were excluded. We employed the MissForest nonparametric approach to impute the remaining missing data for the remaining 470 lipids. Probability Quotient Normalization (PQN) and subsequent log2 transformation were performed, followed by correction for batch effects using a linear model implemented in Limma.^[26,27] Principal component analysis (PCA) was used to ensure successful elimination of batch effects before proceeding with the analyses.

We performed binary comparisons using Volcano plots between hepatic steatosis histology scores 2–3 versus 0–1, lobular inflammation scores 2–3 versus 0–1, ballooning degeneration scores 2 versus 0–1, liver fibrosis stages 3–4 versus 0–2, and genetic variant carrier versus noncarrier status for *PNPLA3* rs738409^{CC/CG} vs. ^{GG}, *TM6SF2* rs58542926^{CC/CT} vs. ^{TT}, *GPAM* rs2792751^{TT/TC} vs. ^{CC}, *HSD17B13* rs4607179^{CC/CA} vs. ^{AA}, and *MTARC1* rs264243 ^{AA/GA} vs. ^{GG}. Log2 fold changes (Log2 FC), raw and adjusted *p* values using Benjamini–Hochberg correction were calculated using LipidR, an established software package for lipidomics analyses.^[28] Cutoffs at Log2 FC of 1.5 and *p* value of 0.05 were used in generating the Volcano plots. We used Orthogonal Partial Least Squares-Discriminant Analysis (OPLS-DA) to compare liver fibrosis stages 3–4 versus 0–2 using only lipidome information.^[29] Lipid Set Enrichment Analysis (LSEA) was used to identify the lipid class that is significantly enriched or reduced as a group with a false detection rate (FDR) <0.05 in LipidR.

To further analyze the lipid metabolism at the level of acyl chains, we developed a unified acyl chain distribution analysis to interrogate the characteristics of fatty acyl chains, the common and potentially exchangeable constituents of most human lipids (Supplemental Figure S1, <http://links.lww.com/HC9/B983>). For lipids with a defined acyl chain structure by mass spectrometry, we extracted acyl chain length and double bond number to generate a new set of lipid class-specific acyl chain variables. The numbers of unique acyl chains identified from various lipid molecules within the same class were used to generate the bubble plot in Python (Python.org). The Log2 FC values

of each acyl chain within TG, Cer, and PC, the most abundant VLDL lipids, were plotted by the acyl chain carbon length and number of double bonds to visualize the trend of changes. Additional lipid species were analyzed, with data shown in the supplementary results. Cer was noted to have a significant amount of lipid species with an acyl chain structure poorly defined. We generated a similar plot with total carbon length and double bond number as a sensitivity analysis.

RESULTS

A biopsy-proven NAFLD registry

A total of 162 patients with biopsy-proven MASLD were enrolled in this study (Table 1). In this cohort, the mean age was 56.1, 42% were females, with a mean BMI of 33.7. A total of 28% had a diagnosis of type II diabetes, and 15.5% had stages 3–4 liver fibrosis on the liver biopsy. Carriers of high-risk MASLD genetic risk factors

TABLE 1 Patient characteristics

Age, y	56.1 (12.9)
Gender, female	68 (42%)
BMI	33.7 (6.5)
Type 2 diabetes mellitus	46 (28%)
MASH histology features	
Hepatic steatosis score	2.0 (0.7)
Inflammation score	1.3 (0.5)
BD score	1.2 (0.7)
Fibrosis score	
0	50 (31%)
1	39 (24%)
2	48 (30%)
3	15 (9%)
4	10 (6%)
Genetic variants	
PNPLA3 (rs738409)	59 (37%)/68 (43%)/31 (20%)
CC/GC/GG	
TM6SF2 (rs58542926)	128 (81%)/28 (18%)/2 (1.3%)
CC/CT/TT	
GPAM (rs2792751)	70 (45%)/65 (42%)/20 (13%)
CC/TC/TT	
HSD17B13 (rs4607179)	99 (64%)/44 (28%)/12 (7.7%)
AA/CA/CC	
MARC1 (rs2642438)	74 (49%)/65 (43%)/11 (7.3%)
GG/AG/AA	

Note: Data reported as either mean (SD) or count (%).
Abbreviations: BD, ballooning degeneration; BMI, body mass index; MASH, metabolic dysfunction–associated steatohepatitis.

were common, with 63% *PNPLA3* rs738409 (C > G), 19% *TM6SF2* rs58542926 (C > T), 55% *GPAM* rs2792751 (C > T), 36% *HSD17B13* rs4607179 (A > C), and 50% *MTARC1* rs2642438 (G > A).

VLDL-lipidomics measurement and data quality control

VLDL isolated from fasting serum was analyzed by mass spectrometry (Figure 2A). The peak intensities of individual lipid species were adjusted by VLDL particle concentration measured by NMR profiling to determine the relative lipid concentration per VLDL particle. After removing data that does not meet the quality control criteria and correcting batch effects through Limma algorithm, a total of 1514 lipid species in 46 lipid classes were discovered, among which lipid classes with the most diverse species were TG, ceramide (Cer), and phosphatidylcholine (PC) (Figure 2B). Lipid classes that provided the highest mass spec total peak intensities were PC, TG, and sphingomyelin (SM) (Supplemental Figure S2, <http://links.lww.com/HC9/B983>). Notably, the mass spec signal intensity does not equal actual lipid concentration, it enables comparison among samples within the same lipid class. Most lipid species have one or more hydrocarbon acyl groups, which are potentially exchangeable across lipid species, while a minority of lipids carry hydrocarbon alkyl groups through an ether bond. We devised a unified acyl chain distribution analysis to better capture the lipidomic signature on the acyl chain level. In the acyl chain distribution analysis, TG, Cer, and PC demonstrated distinct acyl chain compositions (Figure 2C). While the most abundant acyl chains were from palmitic acid (C16:0), palmitoleic acid (C16:1), and oleic acid (C18:1) in TG, fatty acyl chains from lignoceric acid (C24:0) was the most abundant in Cer, and polyunsaturated fatty acids (C18:2, C18:3, C20:4, and C22:6) were abundant in PC. Diacylglycerol (DG), phosphatidylethanolamine (PE), and phosphatidylinositol (PI) had similar acyl chain patterns as PC (Supplemental Figure S3, <http://links.lww.com/HC9/B983>). Surprisingly, the SM acyl chain pattern was quite different from Cer by having predominantly 18 or 20 carbon unsaturated acyl chains. Meanwhile, lyso-phosphatidylcholine (LPC) differed from other PLs in that it had more saturated acyl chains.

Lipidomic features associated with steatohepatitis

Hepatic steatosis impacts the VLDL particle number and sizes produced by the liver.^[19] Herein, we observed a significant impact of hepatic steatosis on

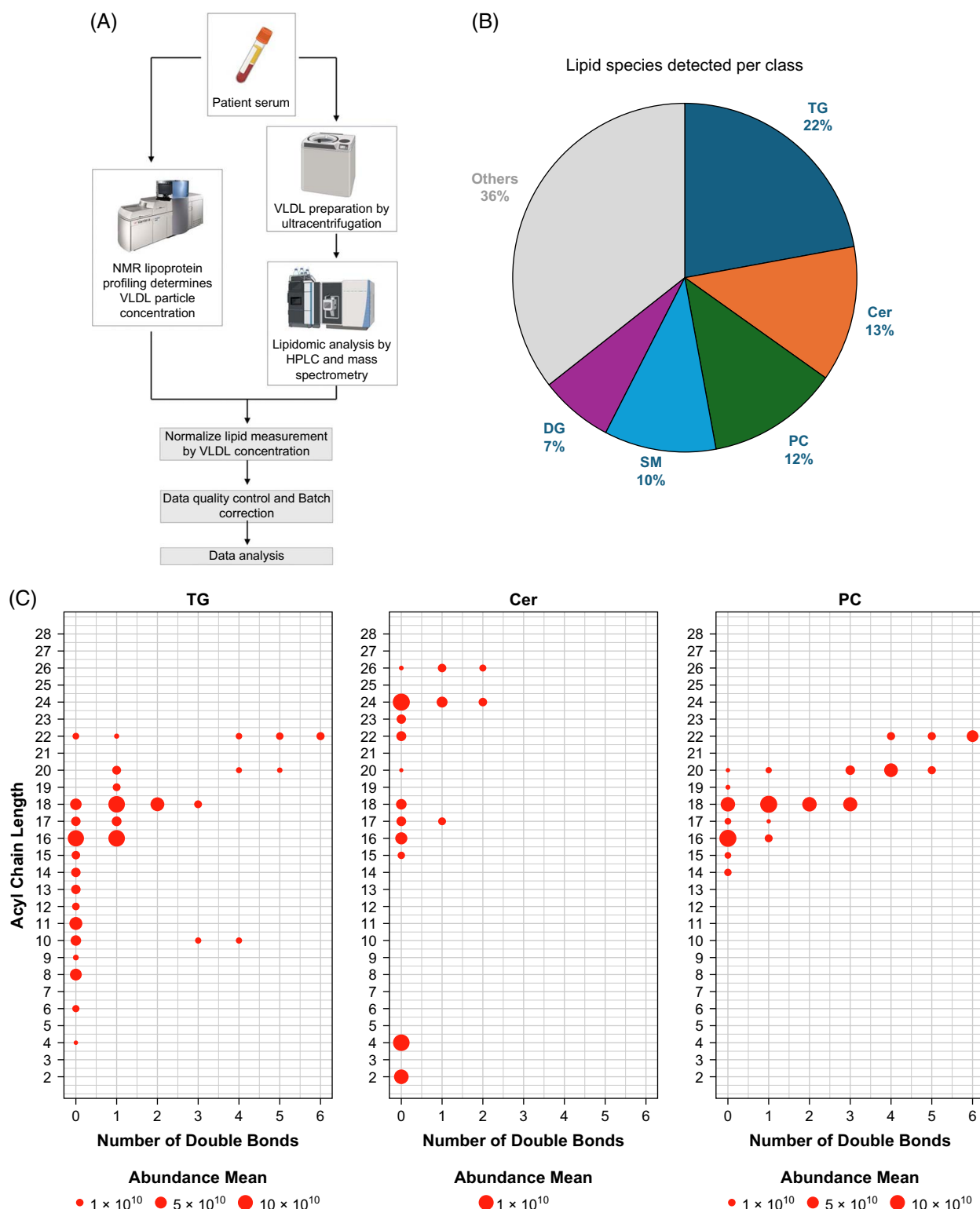


FIGURE 2 VLDL-lipidomics study design and data summary. (A) Flowchart of VLDL-lipidomics analysis. Patient serum is analyzed by NMR lipoprotein profiling to determine the VLDL particle concentration. A fraction of the same serum is ultracentrifuged to isolate VLDL. After lipid extraction, lipids are analyzed by HPLC-mass spectrometry. VLDL-lipidome per VLDL particle is used for analysis after normalization by VLDL concentration. (B) The diagram summarizes the number of lipid species detected in each lipid class. The top 5 lipid classes are TG, Cer, PC, SM, and DG. (C) Bubble plot of the lipid species in TG, Cer, and PC, with the size of the bubble corresponding to mean mass spec signal intensity. Abbreviations: Cer, ceramide; DG, diacylglycerol; HPLC, high-performance liquid chromatography; NMR, nuclear magnetic resonance; PC, phosphatidylcholine; SM, sphingomyelin; TG, triglyceride.

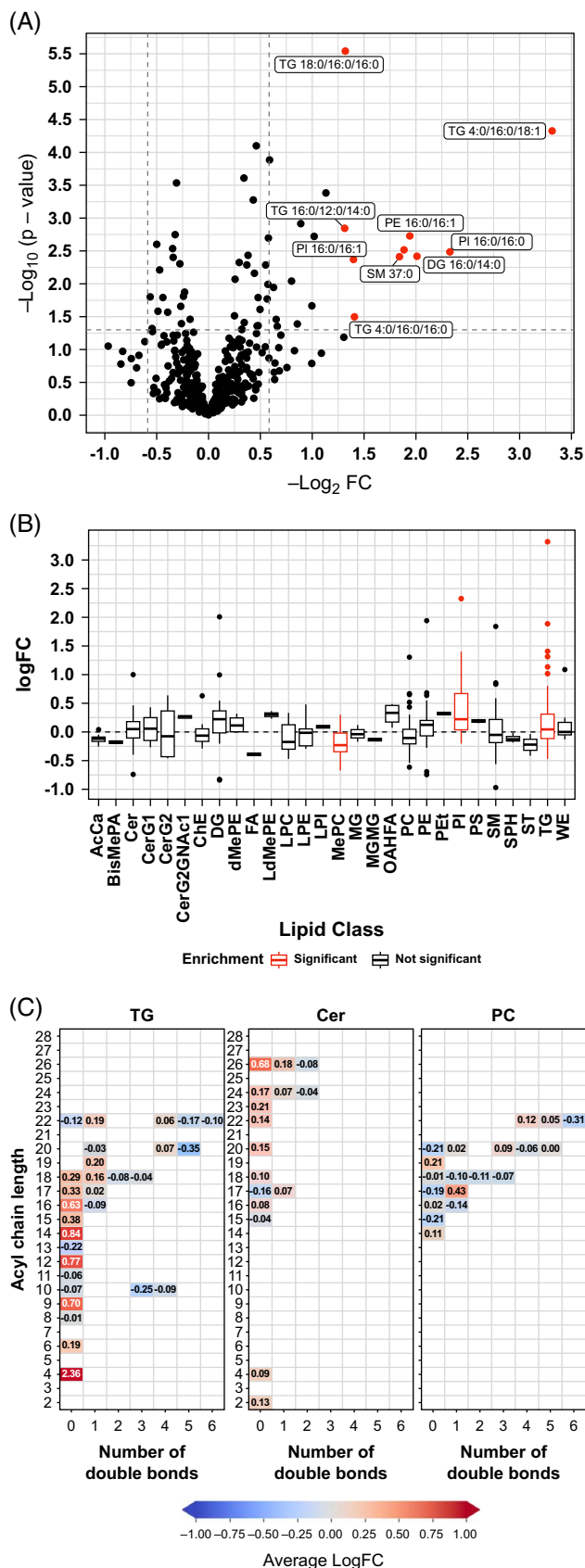


FIGURE 3 VLDL-lipidomic signatures of hepatic steatosis. (A) Volcano plot comparing hepatic steatosis histology score 2–3 versus 1. Cutoff lines representing \log_2 FC > 0.5 or < -0.5, and $p < 0.05$. The

top 10 differentially enriched lipids are shown in red. (B) Lipid set enrichment analysis comparing hepatic steatosis histology score 2–3 versus 1. Statistically enriched or reduced lipid classes are shown in red. (C) Acyl chain distribution analysis for TG, Cer, and PC plotted by the number of carbon and double bonds in the acyl chain. The number represents the \log_2 FC change between hepatic steatosis histology score 2–3 versus 1, with positive changes in red and negative in blue. Abbreviations: Cer, ceramide; \log_2 FC, \log_2 fold changes; PC, phosphatidylcholine; TG, triglyceride.

VLDL-lipidome. Compared to mild steatosis, moderate to severe hepatic steatosis (histological score 2 or 3) was associated with significant increases of 20 lipid species across diverse lipid classes, including TG, PI, PE, DG, and SM (Figure 3A). Interestingly, acyl chains from palmitic acid (C16:0) were noted in most enriched lipids. In lipid class enrichment analysis, moderate to severe hepatic steatosis was associated with statistically significant enrichments in TG, PI, and monoether phosphatidylcholine (MePC) (Figure 3B). Among TG, there was a robust upregulation of TG with saturated acyl chains from butyric (C4:0), lauric (C12:0), myristic (C14:0), and palmitic acid (C16:0), nonessential fatty acids that can be synthesized in hepatocytes (Figure 3C). There was also an enrichment of acyl chain from pelargonic acid (C9:0), a plant-derived fatty acid used for flavoring and also as a pesticide.^[30] Among ceramides, there were interesting reductions in 15–18 carbon acyl chains but reciprocal increases in very long chain fatty acids (Figure 3C). In contrast, no significant acyl chain trends were noted in PC.

Similar analyses were performed for histological scores of lobular inflammation and ballooning degeneration. Significant lobular inflammation (histological score 2 or 3) was associated with enrichment of 4 and reductions of 18 lipid species (Figure 4A). Among a diverse group of lipids with reduced concentration, there was a notable overrepresentation of lipids containing acyl chains from docosahexaenoic acid (C22:6), derived from essential polyunsaturated fatty acids (Figure 4A). Although no lipid classes reached statistically significant enrichment, acyl chain distribution analyses revealed interesting patterns of changes (Figure 4B). For instance, in TG, there were robust reductions in acyl chains from polyunsaturated fatty acids, but increases in saturated acyl chains (Supplemental Figure S4, <http://links.lww.com/HC9/B983>). Small changes associated with significant ballooning degeneration compared to mild ballooning (histology score 2 vs. 0–1) were noted on the Volcano plot (Figure 4C). There was an enrichment of PE in lipid set enrichment analysis (Figure 4D). Acyl chain distribution in TG, Cer, and PC associated with significant ballooning degeneration was similar to that associated with moderate to severe steatosis (Supplemental Figure S5, <http://links.lww.com/HC9/B983>).

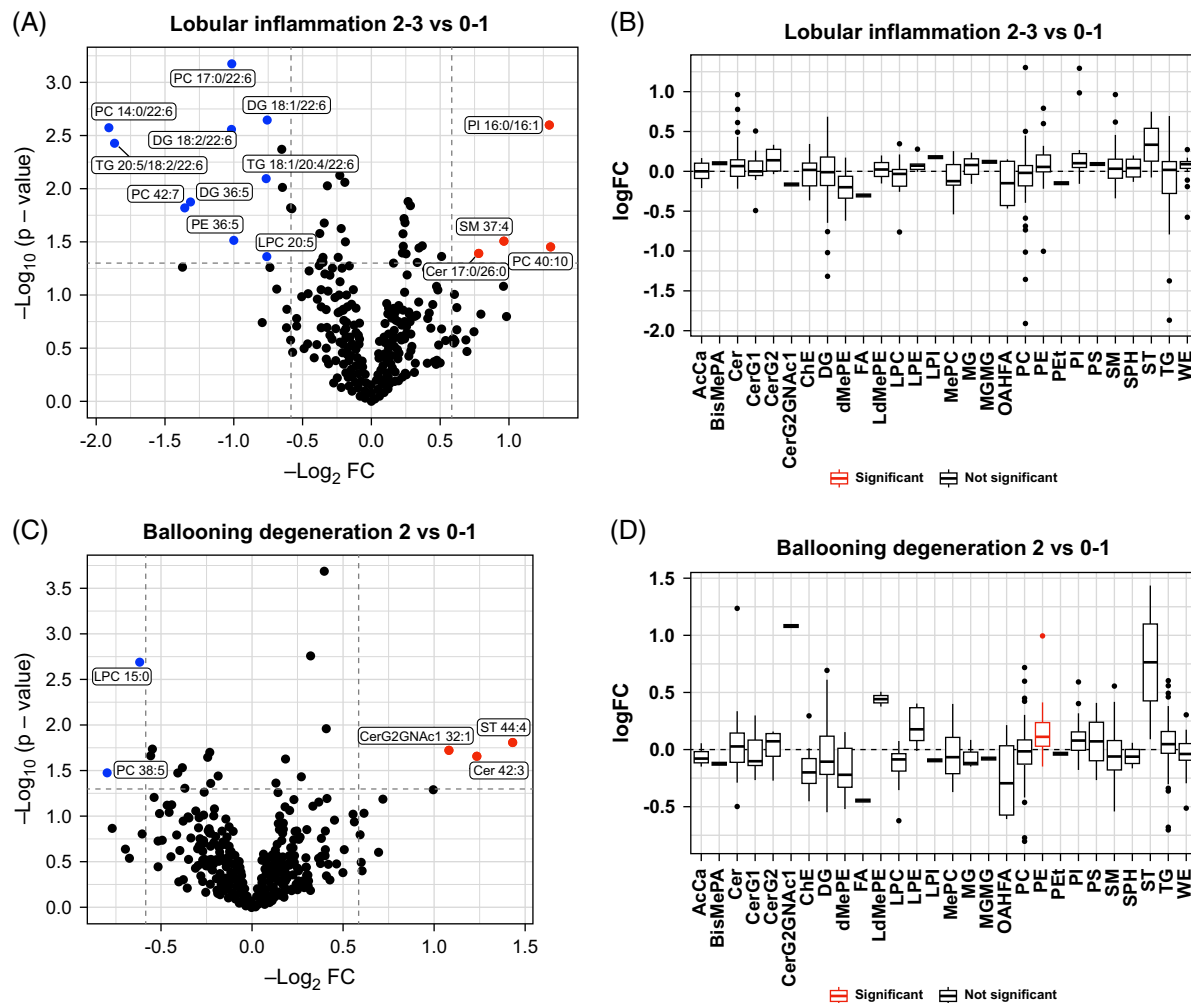


FIGURE 4 VLDL-lipidomic signatures of lobular inflammation and ballooning degeneration. Volcano plots are shown to compare lobular inflammation histology score 2–3 versus 0–1 (A) and ballooning degeneration histology score 2 versus 0–1 (B). Cutoff lines representing $\log_2 FC > 0.5$ or < -0.5 , and $p < 0.05$. The top 10 differentially enriched lipids are shown in red, and reduced lipids are in blue. Lipid set enrichment analyses are performed to compare lobular inflammation histology score 2–3 versus 0–1 (C) and ballooning degeneration histology score 2 versus 0–1 (D). Statistically enriched or reduced lipid classes are shown in red. Abbreviation: $\log_2 FC$, \log_2 fold changes.

Lipidomic features associated with fibrosis

While hepatic steatosis is expected to impact VLDL-lipid directly, the impact of hepatic fibrosis is indirect. Volcano plot demonstrated 11 enriched and 9 reduced lipid species in association with advanced fibrosis (stages 3–4) (Figure 5A). Although there were reductions in some lipids with unsaturated acyl chains as seen in the analyses of lobular inflammation, the overall pattern was far more complex. Lipid set enrichment analyses identified a significant increase in Cer and a reduction in DG (Figure 5B). There were also trends of enrichment in dihexosylceramide (CerG2), dihexosyl N-acetylhexosyl ceramide (CerG2-GNAc1), sterol (ST), PE, PI, and reductions in cholesteryl ester, LPC, and SM. Although these changes do not reach statistical significance, the concordant directions of changes suggest potential alterations in ceramide modification, cholesterol

esterification, and ER membrane integrity. Patients with advanced liver fibrosis form a distinct cluster from those with early fibrosis (stages 0–2) using orthogonal partial least squares-discriminant analysis (OPLS-DA), suggesting VLDL-lipidome could be used to distinguish those with advanced liver fibrosis (Figure 5C). In acyl chain distribution analyses of main lipid classes, advanced liver fibrosis was associated with reductions in TGs with polyunsaturated and short-to-medium length acyl chains, while acyl chains from lauric (C12:0) and myristic (C14:0) remained increased, as in moderate to severe hepatic steatosis (Figure 5D). The reduction of polyunsaturated acyl chains was also seen in PC. Among Cer, most species with saturated or monounsaturated acyl chains showed an enrichment. Notably, acyl chain distribution patterns in major lipid classes associated with advanced liver fibrosis significantly differed from those of moderate-to-severe steatosis.

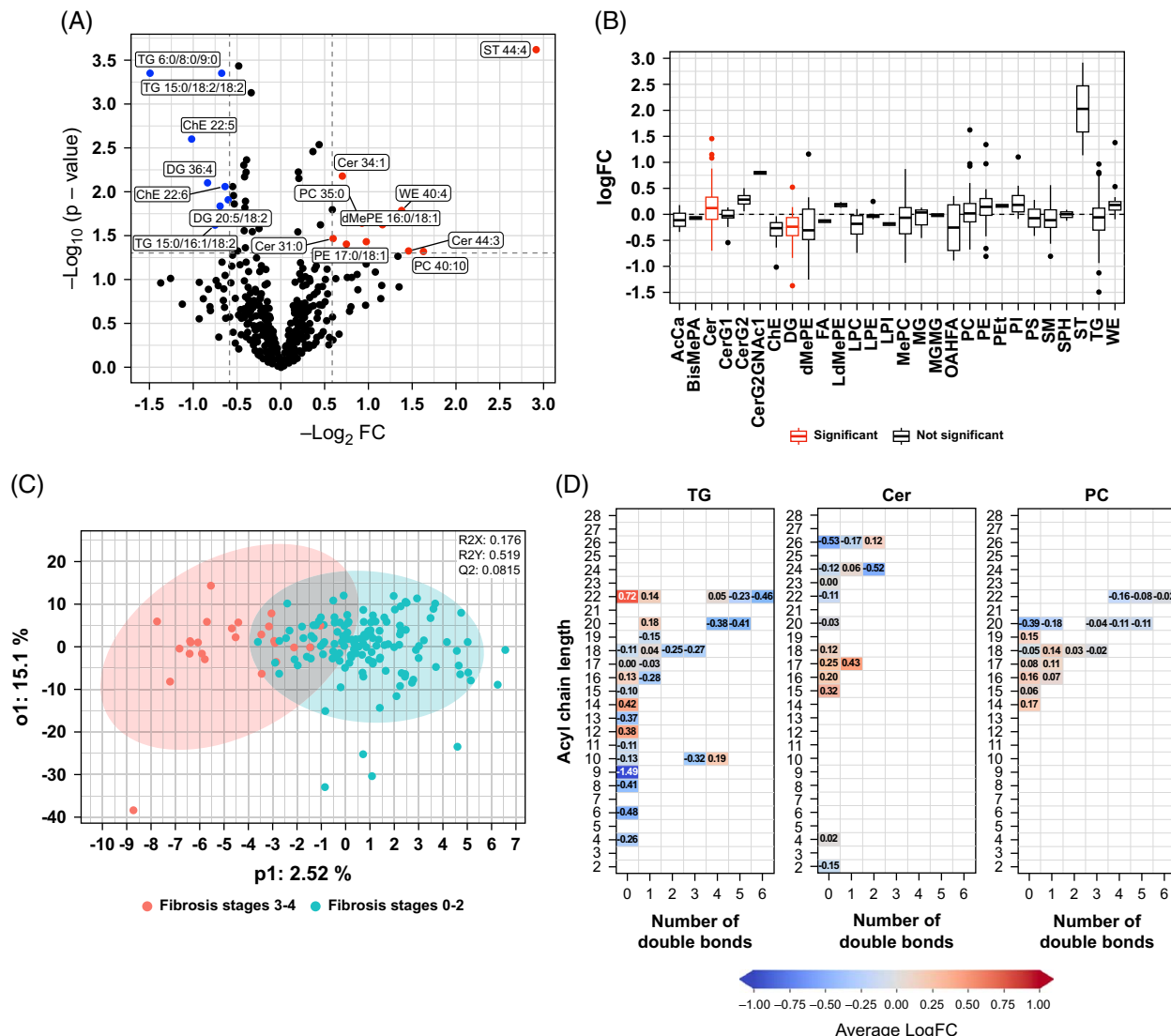


FIGURE 5 VLDL-lipidomic signatures of liver fibrosis. (A) Volcano plot comparing liver fibrosis stages 3–4 versus 0–2 on the liver biopsy. Cutoff lines representing $\log_2 FC > 0.5$ or < -0.5 , and $p < 0.05$. The top 10 differentially enriched lipids are shown in red, and reduced lipids are shown in blue. (B) Lipid set enrichment analysis comparing liver fibrosis stages 3–4 versus 0–2. Statistically enriched or reduced lipid classes are shown in red. (C) Orthogonal partial least squares-discriminant analysis (OPLS-DA) differentiating liver fibrosis stages 3–4 (red) versus 0–2 (cyan). (D) Acyl chain distribution analyses for TG, Cer, and PC plotted by the number of carbon and double bonds in the acyl chain. The number represents the $\log_2 FC$ change between liver fibrosis stages 3–4 versus 0–2, with positive changes in red and negative in blue. Abbreviations: Cer, ceramide; $\log_2 FC$, \log_2 fold changes; PC, phosphatidylcholine; TG, triglyceride.

Lipidomic changes associated with MASLD genetics

Finally, we examined the relationship between VLDL-lipidomics and genetic variants for *PNPLA3* rs738409, *TM6SF2* rs58542926, *GPAM* rs2792751, *HSD17B13* rs4607179, and *MTARC1* rs2642438, as these genes have a link to either lipid or lipoprotein metabolism (Table 2, Figure 6, and Supplemental Figures S6–S10, <http://links.lww.com/HC9/B983>). Although *PNPLA3* rs738409: C > G and *TM6SF2* rs58542926: C > T were both associated with hepatic steatosis, they demonstrated strikingly different VLDL particles and VLDL-lipidomics signatures. *PNPLA3* rs738409^{GG/GC} vs. CC

was associated with increases in VLDL particle concentration and polyunsaturated acyl chains but decreases in VLDL particle sizes (Table 2, Figure 6A, and Supplemental Figures S6 and S7, <http://links.lww.com/HC9/B983>). A comparison between homozygous phenotypes (*PNPLA3* rs738409^{GG} vs. CC) as a sensitivity analysis showed similar results (Supplemental Figure S11, <http://links.lww.com/HC9/B983>). In contrast, *TM6SF2* rs58542926^{TT/TC} vs. CC was associated with an opposite trend of VLDL particle characteristics, a robust and consistent reduction in all TG with monounsaturated and polyunsaturated acyl chains, a signature that was different from other examined genetic variants. While *GPAM* rs2792751: C > T,

TABLE 2 Demographics, histology features, and VLDL characteristics by genetic variants

		Demographics			Histology score				VLDL characteristics	
Genotypes	Number	Age	Sex (%F)	BMI	HS score	LI score	BD score	Fibrosis stages	VLDL conc. (nmol/L)	VLDL size (nm)
PNPLA3 rs738409										
CC	59	57 (12)	42%	34.0 (7.0)	1.8 (0.7)	1.3 (0.5)	1.1 (0.8)	1.2 (1.3)	184.8 (82.3)	52.6 (10.0)
GG/CG	99	55 (14)	41%	33.8 (6.5)	2.1 (0.6)	1.4 (0.6)	1.3 (0.7)	1.4 (1.1)	205.9 (81.4)	51.6 (8.4)
TM6SF2 rs58542926										
CC	128	57 (13)	41%	34.1 (6.5)	1.9 (0.6)	1.3 (0.5)	1.2 (0.7)	1.3 (1.2)	203.0 (82.7)	51.7 (9.0)
TT/TC	30	57 (13)	47%	33.1 (6.3)	2.2 (0.8)	1.4 (0.5)	1.4 (0.7)	1.6 (1.3)	181.3 (80.7)	53.2 (9.4)
GPAM rs2792751										
CC	70	57 (12)	47%	34.0 (6.3)	1.9 (0.6)	1.2 (0.5)	1.1 (0.7)	1.4 (1.2)	196.9 (95.6)	50.1 (7.9)
TT/TC	85	55 (14)	35%	33.6 (6.8)	2.1 (0.7)	1.4 (0.5)	1.3 (0.7)	1.4 (1.2)	197.2 (72.5)	53.0 (9.5)
HSD17B13 rs4607179										
AA	99	57 (13)	45%	33.6 (6.9)	1.9 (0.7)	1.3 (0.5)	1.3 (0.7)	1.5 (1.3)	202.4 (84.9)	51.4 (9.1)
CC/CA	56	54 (12)	32%	33.9 (5.9)	2.1 (0.6)	1.3 (0.5)	1.2 (0.7)	1.2 (1.0)	187.8 (80.7)	52.3 (8.8)
MTARC1 rs2642438										
GG	74	56 (12)	42%	34.4 (7.3)	1.9 (0.7)	1.4 (0.5)	1.3 (0.7)	1.6 (1.3)	196.7 (77.0)	52.3 (9.3)
AA/GA	76	56 (12)	39%	33.1 (5.9)	2.0 (0.6)	1.3 (0.6)	1.2 (0.8)	1.2 (1.1)	194.8 (90.8)	50.7 (8.0)

Note: Values are reported as mean (SD).

Abbreviations: BD, ballooning degeneration; HS, hepatic steatosis; LI, lobular inflammation.

HSD17B13 rs4607179: A > C, and *MTARC1* rs2642438 G > A had similar VLDL-TG signatures, they differ in Cer and PC compartments. In the Cer compartment, *GPAM* rs2792751^{CT/TT vs. CC} and *HSD17B13* rs4607179^{CC/CA vs. AA} were associated with reductions in most Cer species, whereas *PNPLA3* rs738409^{GG/CG vs. CC} and *TM6SF2* rs58542926^{TT/TC vs. CC} again demonstrated contrasting signatures (Figure 6B). The genetic variants associated with Cer patterns appeared to be linked to acyl chain length, which may suggest differential ceramide synthase (CerS) activities, as CerS isoforms have distinct acyltransferase kinetics over acyl chains of different lengths.^[31] In the PC compartment, *MTARC1* rs2642438^{AA/GA vs. GG} was associated with a unique signature of reductions in almost all VLDL-PC species, whereas signatures associated with other genetic variants were not apparent (Figure 6C). To evaluate whether these associations are related to ancestry, we performed sensitivity analyses among non-Hispanic Caucasians and observed very similar associations between genetics and differential lipid enrichment (Supplemental Figure S12, <http://links.lww.com/HC9/B983>).

DISCUSSION

Hepatic steatosis in MASLD is characterized by the accumulation of intracellular lipid droplets, presumably driven by altered hepatocellular lipid homeostasis. VLDL shares a similar structure to intracellular lipid droplets and derives much of its lipids directly from

hepatocellular lipid droplets. Our study demonstrates that VLDL-lipidomics is a powerful tool to interrogate hepatocellular lipid homeostasis in humans.

Biological relevance of VLDL-lipidomics

The biology of VLDL underscores the interpretation of VLDL-lipidomics and its relevance to hepatocellular lipid metabolism. The lipid cargo of VLDL derives from both the ER and Golgi membrane and intracellular lipid droplets (Figure 1). The production of VLDL involves an exceptionally complex interplay among protein, lipid constituents, chaperones, and transporters in the ER and Golgi apparatus.^[4,16,32] Although some details of this cellular process remain to be clarified, the current framework of VLDL synthesis suggests that the composition of VLDL-lipidome will largely mirror the lipidome of cellular organelle where VLDL lipids are originated as the incorporation of lipids into VLDL is largely driven by lipid availability and is agnostic to acyl chain characteristics. Experimentally, Donnelly et al^[33] demonstrated using isotope labeling that VLDL-TG highly represents TG in the human liver in MASLD. Density centrifugation-based lipoprotein isolation was perfected half a century ago and has been used in lipidomics studies for cardiovascular diseases.^[34] Lipoprotein lipidome has been used to study insulin resistance, a main pathogenic driver in MASLD.^[35] Luukkonen et al^[6] have analyzed VLDL-lipidome to probe the biology of *TM6SF2* in MASLD. As the most comprehensive effort so far to study VLDL-lipidomics in

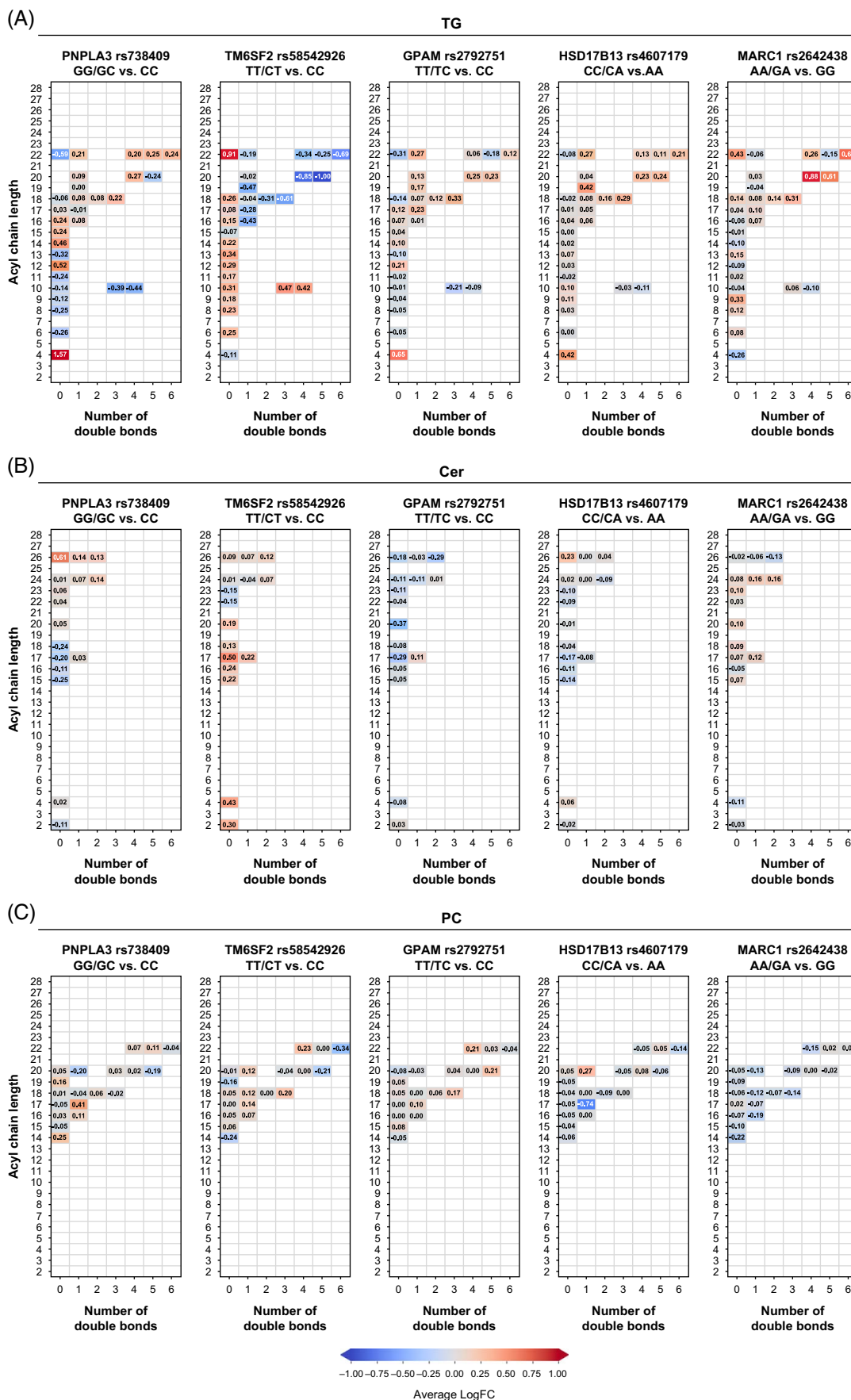


FIGURE 6 VLDL-lipidomic signatures of MASLD genetics. Acyl chain distribution analyses for TG (A), Cer (B), and PC (C) plotted by the number of carbon and double bonds in the acyl chain showing differences between the following annotated genotypes: *PNPLA3* rs738409^{GG/GC} vs. ^{CC}, *TM6SF2* rs5842926^{TT/CT} vs. ^{CC}, *GPAM* rs2792751^{TT/TC} vs. ^{CC}, *HSD17B13* rs4607179^{CC/CA} vs. ^{AA}, and *MTARC1* rs2642438^{AA/GA} vs. ^{GG}. The number represents the Log2 FC change between liver fibrosis stages 3–4 versus 0–2, with positive changes in red and negative in blue. Abbreviations: Cer, ceramide; Log2 FC, Log2 fold changes; MASLD, metabolic dysfunction–associated steatotic liver disease; PC, phosphatidylcholine; TG, triglyceride.

MASLD, we have made 2 innovations. First, we normalized the VLDL-lipidome by the VLDL particle concentration measured by NMR lipid profiling to determine the lipidome per VLDL particle. This method, to a large extent, eliminates the bias related to VLDL particle concentration that can be influenced by the number of viable hepatocytes and is subject to changes with fibrogenesis. Second, we developed a unified acyl chain distribution analysis across different lipid classes. Unlike genomics and proteomics, where study targets are independent and diverse, lipids in lipidomics share a high degree of structural similarity and metabolic pathways. The acyl chain distribution analysis reveals features of lipid profile changes related to chain length and number of double bonds that are often not captured by lipid set enrichment analysis or binary differential expression analysis (eg, Volcano plot). Our observation does not support the premise that acyl chains are freely exchangeable. Rather, acyl chains in different lipid classes often display discordant pattern changes in relationship to genetics or pathogenic factors, suggesting the presence of class-specific lipid compartments and metabolic pathways. Notably, among VLDL lipid classes, disease-related and genetics-related acyl chain signatures were more prominent in TG and Cer than PLs, suggesting MASLD may perturb lipids differently by class.

Relationship between hepatic steatosis and VLDL-lipidome in MASLD

Hepatic steatosis is expected to augment VLDL lipidation, leading to increased TG content in VLDL particles. Human kinetic studies demonstrated a direct link between intrahepatic TG and VLDL production.^[36] An estimate based on these measurements indicates that in 70 kg men with 5% intrahepatic TG, daily VLDL production accounts for about 15% of the intrahepatic TG. Higher intrahepatic TG leads to an increase in VLDL-TG production, but this compensatory response of VLDL-TG production plateaus at 15% intrahepatic TG content in female and 25% in male.^[36] We and others have shown that intrahepatic steatosis in MASLD is associated with increased VLDL particle number and larger VLDL particle sizes in the circulation.^[19,36] As expected, the VLDL-lipidome in moderate to severe steatosis demonstrates an enrichment in TG compared to mild steatosis. But not all TG were enriched equally.

Most enriched TG carried saturated acyl chains (Figure 3A). Among abundant acyl chains in VLDL-TG, acyl chains from palmitic acid (C16:0) had the most significant enrichment, while those from palmitoleic (C16:1) and oleic acid (C18:1) showed no significant increases. Polyunsaturated acyl chains were in fact reduced. These acyl chain patterns could be specific to steatosis driven by metabolic dysfunction. The reduction of TG with polyunsaturated acyl chains has been reported in the MASLD liver tissue, supporting the validity of VLDL-lipidomics as a tool to study lipid changes in human liver cells.^[37]

Impact of hepatocellular dysfunction on VLDL-lipidome in advanced fibrosis

Lipid and lipoprotein homeostasis could be altered under impairment of hepatocellular function, such as ballooning degeneration and liver fibrosis. We and others have shown impaired cholesterol metabolism in alcohol-associated hepatitis and acute on chronic liver failure.^[38,39] Hepatocellular dysfunction likely also occurs during progressive liver fibrosis. This premise was supported by a reduction in fasting TG and VLDL particles in association with liver fibrosis or cirrhosis.^[40–42]

VLDL-lipidomics revealed complex fibrosis-associated changes that may suggest impaired hepatocellular lipid metabolism. Indeed, advanced liver fibrosis demonstrates a decrease in TG species predominantly among those with polyunsaturated acyl chains (Figure 5D). In PC and Cer groups, a similar trend of reduction in long (C > 20) and polyunsaturated acyl chains was noted along with a relative preservation of medium length acyl chains (C14–18). While steatosis had a discordant impact on acyl chain characteristics among TG, PC, and Cer (Figure 3C), liver fibrosis had a concordant impact on acyl chain characteristics across these 3 major lipid classes. One possible explanation is a loss of lipid compartmentation, resulting in a higher degree of acyl-CoA substrate sharing. Liver fibrosis was associated with an enrichment of ceramide (Figure 5B), which was in part driven by a group of ceramides with very high carbon numbers. These ceramides with very high carbon numbers likely represent acylceramides, lipids with an additional acyl chain modification, rendering increased hydrophobicity to enter the core of lipid droplets.^[43] There was also a trend of increase in CerG2 and

CerG2GNAc1 (Figure 5B). Previous studies have associated the accumulation of glycosphingolipids with the development of HCC.^[44] Although free cholesterol was not captured in our study, VLDL-lipidomics revealed a trend of reduction in cholesteryl ester but an increase in sterol (ST), suggesting a potential reduction in cholesterol acyltransferase activity. Furthermore, VLDL-PE was significantly enriched in patients with significant ballooning degeneration (histology score 2 vs. 0–1) (Figure 4D). In advanced fibrosis, VLDL-PE and VLDL-PI levels trended higher, while sphingomyelin (SM) levels trended higher in advanced fibrosis. Typically, PC and SM are on the inner leaflet of the ER membrane, more accessible to the VLDL assembly machinery, while PE and PI are on the outer leaflet of the ER and are not as accessible. This trend may suggest a disruption of the biological ER membrane integrity in association with advanced fibrosis.

While VLDL-lipidomic changes associated with ballooning degeneration were similar to those of advanced fibrosis in both lipid classes and acyl chain characteristics, a distinct VLDL-lipidomic signature is associated with lobular inflammation. The reduction in polyunsaturated acyl chains, such as arachidonic (C20:4), eicosapentaenoic (C20:5), and docosahexaenoic acid (C22:6) was striking (Supplemental Figure S4, <http://links.lww.com/HC9/B983>). Of note, these acyl chains derive from essential polyunsaturated fatty acids that can only be acquired through dietary sources. As lobular inflammation involves immune cells, this finding may suggest a possible causal implication of polyunsaturated fatty acids in immune regulation.

Impact of MASLD genetics on VLDL-lipidome

VLDL-lipidomics revealed the impact of MASLD-related genetics on the hepatocellular lipidome. Among the 5 studied MASLD-related genetic variants, variants in *PNPLA3*, *TM6SF2*, and *GPAM* were associated with both hepatic steatosis and liver injury, while variants in *HSD17B13* and *MTARC1* were associated with protection against liver injury.^[5,7,8,11–13] The observations in VLDL-lipidomics support previous studies on the impact of these genetic variants. In comparisons between carrier versus noncarrier, patients with *PNPLA3*, *TM6SF2*, and *GPAM* variants had worse steatosis scores along with scores in lobular inflammation, ballooning, and fibrosis, while those with *HSD17B13* and *MTARC1* variants demonstrated trends toward lower scores on inflammation, ballooning, and fibrosis (Table 2).

PNPLA3 r738409 C > G polymorphism is a major risk factor for steatotic liver disease that is independent of

metabolic dysfunction.^[7,45] VLDL-TG in *PNPLA3* variant carriers showed fatty acyl chain signatures that is different from that is associated with steatosis in MASLD (Figure 6).^[45] A recent study suggested that *PNPLA3* is a triglyceride lipase that functions to mobilize polyunsaturated fatty acids to PLs, while polyunsaturated PLs facilitate efficient VLDL production.^[46] A study by Luukkonen et al^[47] compared fatty acid compositions in VLDL-TG between *PNPLA3* r738409 GG versus CC carriers. Our observations are largely concordant with theirs in increases of stearic (16:0), arachidonic acids (20:4), and reductions in linoleic (18:2), linolenic (18:3), eicosapentaenoic (20:5), and Cervonic acids (22:6) (Supplemental Figure S11, <http://links.lww.com/HC9/B983>).

TM6SF2, a membrane protein located on the ER and Golgi membrane of hepatocytes, has been directly implicated in VLDL synthesis.^[48] We observed a significant reduction in VLDL-TG with unsaturated acyl chains and a reciprocal increase in TG with saturated acyl chains along with ceramide. Notably, Luukkonen et al^[6] made similar observations using liver tissue, and postulated that *TM6SF2* could function to incorporate polyunsaturated fatty acids into PC and TG in hepatocytes, as such *TM6SF2* genetic variant impairs VLDL production and facilitates hepatic steatosis. These insights were validated in Huh7 cells, a hepatoma cell line in vitro.^[6,49] Together, these observations further support the premise that the mobilization of polyunsaturated fatty acids in TG may be crucial in regulating hepatic steatosis. Nonetheless, it is interesting that the VLDL-PC compartment showed no reciprocal changes, which was also noted by others.^[6,46]

Carriers of *HSD17B13* and *MTARC1* variants, 2 genotypes associated with protection against liver injury, had increases in VLDL-TG with polyunsaturated acyl chains (Figure 6), again underscoring a potential mechanism involving the mobilization of polyunsaturated fatty acids in TG. Carriers of the *MTARC1* variant showed mild but concordant decreases in PC with almost all acyl chain configurations (Figure 6). Interestingly, the liver tissue of *MTARC1* carriers had increases in hepatic PC, suggesting a potential causal link due to reduced VLDL-PC secretion.^[50] The correlation between findings in genetics-associated liver tissue and VLDL-lipidomic signatures underscores VLDL as a circulating instrument to study lipid metabolism in liver cells.

Clinical implications in MASLD

VLDL-lipidomics provides rich observations that inform disease phenotypes and, in some cases, sheds light on pathogenesis. For instance, hepatic steatosis is associated with an increase in saturated fatty acids, but not

polyunsaturated fatty acids such as linoleic (C18:2), linolenic (C18:3), arachidonic (C20:4), and eicosapentaenoic acids (C20:5). As mammals lack ω 3 and ω 6 desaturases, polyunsaturated long chain fatty acids must be obtained from diet. The disproportional increase in nonessential fatty acids associated with hepatic steatosis suggests that de novo lipogenesis is the main driver for hepatic steatosis. Second, the reduction in polyunsaturated VLDL-TG appears to be linked to MASLD. Both advanced fibrosis and the *TM6SF2* variant are associated with a reduction in polyunsaturated VLDL-TG, while protective genetic variants such as those in *HSD17B13* and *MTARC1* are associated with increases in polyunsaturated VLDL-TG. This observation sheds light on the biology and pathogenesis of MASLD and raises the possibility that a diet rich in polyunsaturated fatty acids will be of benefit in managing MASLD.

Contextual consideration and limitations

Some limitations need to be considered when interpreting current observations. First, this study cohort included only patients with MASLD and lacked healthy controls. Caution is needed to extend the interpretation derived from varying degrees of disease severity to healthy individuals. Second, our lipidomics used mass spectrometry, in which signal intensity is influenced by the efficiency of ionization and does not represent actual lipid concentration. It is reasonable to compare lipid concentration within the same lipid class, but not across classes. Furthermore, some lipid species were not captured in the current platform, such as free cholesterol, fatty acids, etc. Finally, the current algorithm failed to define all acyl chain structures, and only the total molecule carbon length and double bond number were known for some lipids, especially in the Cer class. Future studies should validate current findings in a larger cohort that includes healthy controls.

In summary, VLDL biology is intimately related to the pathogenesis of MASLD. VLDL-lipidomics informs lipid homeostasis in hepatocytes and captures lipid signatures relevant to metabolic dysfunction-associated steatohepatitis disease features. This study demonstrates that VLDL-lipidome is related to intrahepatic lipid burden, vis-à-vis hepatic steatosis, which promotes VLDL production, and 2 key modifying factors: that is, the functional health of hepatocytes (eg, fibrosis) and genetics that can alter lipid metabolism and lipoprotein synthesis. Understanding this relationship will enable VLDL-lipidomics to be used not only as a research tool, but also potentially as a diagnostic biomarker.

ACKNOWLEDGMENTS

The authors dedicate this publication to the memory of M. Julia Brosnan (July 15, 1963–March 24, 2021),

whose scientific efforts and wisdom made the work possible.

FUNDING INFORMATION

This work is in part supported by NIH grants to Michelle La (K23DK083439), Z. Gordon Jiang (K08DK115883, R01AA030770), and a Pfizer research grant to Michelle La and Z. Gordon Jiang.

CONFLICTS OF INTEREST

Aaron Hakim consults for Deep Track Capital, LP. Aaron Hakim and Z. Gordon Jiang are members of the Scientific Advisory Board for OliX Pharmaceuticals. Margery A. Connelly is an employee of Labcorp. Melissa R. Miller is an employee of Pfizer. Neither members of Labcorp nor Pfizer were responsible for data analysis.

ORCID

David Guardamino Ojeda  <https://orcid.org/0000-0002-3122-2218>

REFERENCES

1. Younossi ZM, Golabi P, Paik JM, Henry A, Van Dongen C, Henry L. The global epidemiology of nonalcoholic fatty liver disease (NAFLD) and nonalcoholic steatohepatitis (NASH): A systematic review. *Hepatology*. 2023;77:1335–47.
2. Terrault NA, Francoz C, Berenguer M, Charlton M, Heimbach J. Liver Transplantation 2023: Status report, current and future challenges. *Clin Gastroenterol Hepatol*. 2023;21:2150–66.
3. Angulo P. Nonalcoholic fatty liver disease. *N Engl J Med*. 2002;346:1221–31.
4. Jiang ZG, Robson SC, Yao Z. Lipoprotein metabolism in nonalcoholic fatty liver disease. *J Biomed Res*. 2013;27:1–13.
5. Kozlitina J, Smagris E, Stender S, Nordestgaard BG, Zhou HH, Tybjaerg-Hansen A, et al. Exome-wide association study identifies a *TM6SF2* variant that confers susceptibility to nonalcoholic fatty liver disease. *Nat Genet*. 2014;46:352–6.
6. Luukkonen PK, Zhou Y, Nidhina Haridas PA, Dwivedi OP, Hyotylainen T, Ali A, et al. Impaired hepatic lipid synthesis from polyunsaturated fatty acids in *TM6SF2* E167K variant carriers with NAFLD. *J Hepatol*. 2017;67:128–36.
7. Romeo S, Kozlitina J, Xing C, Pertsemlidis A, Cox D, Pennacchio LA, et al. Genetic variation in *PNPLA3* confers susceptibility to nonalcoholic fatty liver disease. *Nat Genet*. 2008;40:1461–5.
8. Abul-Husn NS, Cheng X, Li AH, Xin Y, Schurmann C, Stevis P, et al. A protein-truncating *HSD17B13* variant and protection from chronic liver disease. *N Engl J Med*. 2018;378:1096–106.
9. Pirazzi C, Adiels M, Burza MA, Mancina RM, Levin M, Stahlman M, et al. Patatin-like phospholipase domain-containing 3 (*PNPLA3*) I148M (rs738409) affects hepatic VLDL secretion in humans and in vitro. *J Hepatol*. 2012;57:1276–82.
10. Jiang ZG, Tapper EB, Kim M, Connelly MA, Krawczyk SA, Yee EU, et al. Genetic determinants of circulating lipoproteins in nonalcoholic fatty liver disease. *J Clin Gastroenterol*. 2018;52:444–51.
11. Hakim A, Moll M, Brancale J, Liu J, Lasky-Su JA, Silverman EK, et al. Genetic variation in the mitochondrial glycerol-3-phosphate acyltransferase is associated with liver injury. *Hepatology*. 2021;74:3394–408.
12. Jamialahmadi O, Mancina RM, Ciociola E, Tavaglione F, Luukkonen PK, Baselli G, et al. Exome-Wide Association Study

- on alanine aminotransferase identifies sequence variants in the GPAM and APOE associated with fatty liver disease. *Gastroenterology*. 2021;160:1634–646.e7.
13. Emdin CA, Haas ME, Khara AV, Aragam K, Chaffin M, Klarin D, et al. A missense variant in Mitochondrial Amidoxime Reducing Component 1 gene and protection against liver disease. *PLoS Genet*. 2020;16:e1008629.
 14. Pirola CJ, Sookoian S. The lipidome in nonalcoholic fatty liver disease: Actionable targets. *J Lipid Res*. 2021;62:100073.
 15. Puri P, Wiest MM, Cheung O, Mirshahi F, Sargeant C, Min HK, et al. The plasma lipidomic signature of nonalcoholic steatohepatitis. *Hepatology*. 2009;50:1827–38.
 16. Lee HC, Akhmedov A, Chen CH. Spotlight on very-low-density lipoprotein as a driver of cardiometabolic disorders: Implications for disease progression and mechanistic insights. *Front Cardiovasc Med*. 2022;9:993633.
 17. Mashek DG. Hepatic lipid droplets: A balancing act between energy storage and metabolic dysfunction in NAFLD. *Mol Metab*. 2021;50:101115.
 18. Blanco A, Blanco G. Chapter 15 - Lipid Metabolism. In: Blanco A, Blanco G, editors. *Medical Biochemistry*. Academic Press; 2017: 325–365.
 19. Jiang ZG, Tapper EB, Connelly MA, Pimentel CF, Feldbrugge L, Kim M, et al. Steatohepatitis and liver fibrosis are predicted by the characteristics of very low density lipoprotein in nonalcoholic fatty liver disease. *Liver Int*. 2016;36:1213–20.
 20. Matyus SP, Braun PJ, Wolak-Dinsmore J, Jeyarajah EJ, Shalaurava I, Xu Y, et al. NMR measurement of LDL particle number using the Vantera Clinical Analyzer. *Clin Biochem*. 2014; 47:203–10.
 21. Huffman KM, Parker DC, Bhapkar M, Racette SB, Martin CK, Redman LM, et al. Calorie restriction improves lipid-related emerging cardiometabolic risk factors in healthy adults without obesity: Distinct influences of BMI and sex from CALERIE a multicentre, phase 2, randomised controlled trial. *EClinicalMedicine*. 2022;43:101261.
 22. Wasan KM, Cassidy SM, Kennedy AL, Peteherych KD. Lipoprotein isolation and analysis from serum by preparative ultracentrifugation. *Methods Mol Med*. 2001;52:27–35.
 23. Breitkopf SB, Ricoult SJH, Yuan M, Xu Y, Peake DA, Manning BD, et al. A relative quantitative positive/negative ion switching method for untargeted lipidomics via high resolution LC–MS/MS from any biological source. *Metabolomics*. 2017;13:30.
 24. Das S, Forer L, Schonherr S, Sidore C, Locke AE, Kwong A, et al. Next-generation genotype imputation service and methods. *Nat Genet*. 2016;48:1284–7.
 25. Purcell S, Neale B, Todd-Brown K, Thomas L, Ferreira MA, Bender D, et al. PLINK: A tool set for whole-genome association and population-based linkage analyses. *Am J Hum Genet*. 2007; 81:559–75.
 26. Dieterle F, Ross A, Schlotterbeck G, Senn H. Probabilistic quotient normalization as robust method to account for dilution of complex biological mixtures. Application in 1H NMR metabolomics. *Anal Chem*. 2006;78:4281–90.
 27. Ritchie ME, Phipson B, Wu D, Hu Y, Law CW, Shi W, et al. limma powers differential expression analyses for RNA-sequencing and microarray studies. *Nucleic Acids Res*. 2015;43:e47.
 28. Mohamed A, Molendijk J, Hill MM. lipidr: A software tool for data mining and analysis of lipidomics datasets. *J Proteome Res*. 2020;19:2890–7.
 29. Bylesjö M, Rantalainen M, Cloarec O, Nicholson JK, Holmes E, Trygg J. OPLS discriminant analysis: Combining the strengths of PLS-DA and SIMCA classification. *J Chemom*. 2006;20: 341–51.
 30. European Food Safety Authority; Alvarez F, Arena M, Auteri D, Borroto J, Brancato A, et al. Peer review of the pesticide risk assessment of the active substance pelargonic acid (nonanoic acid). *EFSA J*. 2021;19:e06813.
 31. Raichur S. Ceramide synthases are attractive drug targets for treating metabolic diseases. *Front Endocrinol (Lausanne)*. 2020; 11:483.
 32. Tiwari S, Siddiqi SA. Intracellular trafficking and secretion of VLDL. *Arterioscler Thromb Vasc Biol*. 2012;32:1079–86.
 33. Donnelly KL, Smith CI, Schwarzenberg SJ, Jessurun J, Boldt MD, Parks EJ. Sources of fatty acids stored in liver and secreted via lipoproteins in patients with nonalcoholic fatty liver disease. *J Clin Invest*. 2005;115:1343–51.
 34. Ding M, Rexrode KM. A review of lipidomics of cardiovascular disease highlights the importance of isolating lipoproteins. *Metabolites*. 2020;10:163.
 35. Kotronen A, Velagapudi VR, Yetukuri L, Westerbacka J, Bergholm R, Ekroos K, et al. Serum saturated fatty acids containing triacylglycerols are better markers of insulin resistance than total serum triacylglycerol concentrations. *Diabetologia*. 2009;52:684–90.
 36. Mittendorfer B, Yoshino M, Patterson BW, Klein S. VLDL triglyceride kinetics in lean, overweight, and obese men and women. *J Clin Endocrinol Metab*. 2016;101:4151–60.
 37. Puri P, Baillie RA, Wiest MM, Mirshahi F, Choudhury J, Cheung O, et al. A lipidomic analysis of nonalcoholic fatty liver disease. *Hepatology*. 2007;46:1081–90.
 38. Hu K, Perez-Matos MC, Argemi J, Vilar-Gomez E, Shalaurava I, Bullitt E, et al. Lipoprotein Z, a hepatotoxic lipoprotein, predicts outcome in alcohol-associated hepatitis. *Hepatology*. 2022;75: 968–82.
 39. Claria J, Curto A, Moreau R, Colsch B, Lopez-Vicario C, Lozano JJ, et al. Untargeted lipidomics uncovers lipid signatures that distinguish severe from moderate forms of acutely decompensated cirrhosis. *J Hepatol*. 2021;75:1116–27.
 40. Jiang ZG, Tsugawa Y, Tapper EB, Lai M, Afdhal N, Robson SC, et al. Low-fasting triglyceride levels are associated with non-invasive markers of advanced liver fibrosis among adults in the United States. *Aliment Pharmacol Ther*. 2015;42:106–16.
 41. Jiang ZG, de Boer IH, Mackey RH, Jensen MK, Lai M, Robson SC, et al. Associations of insulin resistance, inflammation and liver synthetic function with very low-density lipoprotein: The Cardiovascular Health Study. *Metabolism - Clinical and Experimental*. 2016;65:92–9.
 42. Fujita K, Nozaki Y, Wada K, Yoneda M, Fujimoto Y, Fujitake M, et al. Dysfunctional very-low-density lipoprotein synthesis and release is a key factor in nonalcoholic steatohepatitis pathogenesis. *Hepatology*. 2009;50:772–80.
 43. Senkal CE, Salama MF, Snider AJ, Allopenna JJ, Rana NA, Koller A, et al. Ceramide 1s metabolized to acylceramide and stored in lipid droplets. *Cell Metab*. 2017;25:686–97.
 44. Byrne FL, Olzomer EM, Lolies N, Hoehn KL, Wegner MS. Update on glycosphingolipids abundance in hepatocellular carcinoma. *Int J Mol Sci*. 2022;23:4477.
 45. Luukkonen PK, Zhou Y, Sadevirta S, Leivonen M, Arola J, Oresic M, et al. Hepatic ceramides dissociate steatosis and insulin resistance in patients with non-alcoholic fatty liver disease. *J Hepatol*. 2016;64:1167–75.
 46. Johnson SM, Bao H, McMahon CE, Chen Y, Burr SD, Anderson AM, et al. PNPLA3 is a triglyceride lipase that mobilizes polyunsaturated fatty acids to facilitate hepatic secretion of large-sized very low-density lipoprotein. *Nat Commun*. 2024;15: 4847.
 47. Luukkonen PK, Nick A, Hölttä-Vuori M, Thiele C, Isokuortti E, Lallukka-Brück S, et al. Human PNPLA3-I148M variant increases hepatic retention of polyunsaturated fatty acids. *JCI Insight*. 2019;4:e127902.
 48. Mahdessian H, Taxiarchis A, Popov S, Silveira A, Franco-Cereceda A, Hamsten A, et al. TM6SF2 is a regulator of liver fat metabolism influencing triglyceride secretion and hepatic lipid droplet content. *Proc Natl Acad Sci U S A*. 2014;111: 8913–8.

49. Ruhanen H, Nidhina Haridas PA, Eskelinen EL, Eriksson O, Olkkonen VM, Kakela R. Depletion of TM6SF2 disturbs membrane lipid composition and dynamics in HuH7 hepatoma cells. *Biochim Biophys Acta*. 2017;1862:676–85.
50. Luukkonen PK, Juuti A, Sammalkorpi H, Penttilä AK, Oresic M, Hyötyläinen T, et al. MARC1 variant rs2642438 increases hepatic phosphatidylcholines and decreases severity of non-alcoholic fatty liver disease in humans. *J Hepatol*. 2020;73:725–6.

How to cite this article: Guardamino Ojeda D, Yalcin Y, Pita-Juarez Y, Hakim A, Bhattarai S, Chen Z, et al. VLDL lipidomics reveals hepatocellular lipidome changes in metabolic dysfunction–associated steatotic liver disease. *Hepatol Commun*. 2025;9:e0716. <https://doi.org/10.1097/HC9.0000000000000716>